

ULTRAVIOLET AND VISUAL SPECTRA OF GAMMA CASSIOPEIAE

RALPH C. BOHLIN*

Princeton University Observatory, Princeton, New Jersey

Received 1970 May 12; revised 1970 June 2

ABSTRACT

A rocket ultraviolet spectrum of γ Cas (B0.5 IVpe) was obtained with a resolution of about 2 Å between 1060 and 2130 Å on 1968 November 15. The strength of the interstellar $L\alpha$ absorption line corresponds to an average density of 0.15 atoms cm^{-3} of neutral hydrogen over the 220 pc to γ Cas, while the absence of any observable lines of molecular hydrogen yielded an upper limit of 2.4×10^{-3} molecules cm^{-3} . Possible interstellar absorption lines of C II, N I, and Si II have widths that indicate that the low-density gas in which the lines arise may have an exponential velocity distribution with a dispersion of $\eta = 15 \text{ km sec}^{-1}$. The C IV line at 1550 Å is the only spectral feature with a P Cygni profile.

OAO and visual spectra covering the wavelength range 1100–5000 Å are also analyzed. The measured amount of Balmer continuous emission can be used to explain the weakness of the He I and other visual photospheric lines if the temperature and optical depth of the circumstellar envelope are known. If γ Cas has an envelope consisting of discrete clouds, each of which has an optical depth of unity at 3647 Å and an electron temperature of 20000° K, then the Balmer continuous emission is accounted for quantitatively and the line profiles in the ultraviolet and visual can be explained qualitatively.

I. INTRODUCTION

Secchi (1867) discovered the first Be star when he observed emission at $H\beta$ in γ Cas in 1866. The star was relatively quiescent until the period 1933–1941, when spectacular changes occurred in its spectrum. The two shell phases in 1935–1936 and 1939–1940 and the preceding intervals of enhanced emission lines are well illustrated by Cowley and Marlborough (1968). Since the peak of the second shell phase in 1940 January, the sharp shell lines have gradually faded away. The visual magnitude brightened to 1.6 in 1936–1937, but by 1942 had faded to 2.6 and remained constant until 1966, when Shelus (1967) reported a return to the pre-1933 value of 2.2.

Since it seemed likely that such an unusual star should have interesting features in the far-ultraviolet, a rocket spectrograph was flown to observe γ Cas. In § II, the features in this ultraviolet spectrum are identified and discussed. Sections III and IV contain similar presentations for recent Orbiting Astronomical Observatory (OAO) scans and for a visual spectrogram of γ Cas. The implications of the data for the interstellar medium and for the star itself are discussed in §§ V and VI, respectively.

II. ROCKET ULTRAVIOLET SPECTRUM

The all-reflective ultraviolet spectrograph described by Morton, Jenkins, and Bohlin (1968) was launched aboard Aerobee 4.268 on 1968 November 15 at 07^h45^m U.T. from the White Sands Missile Range. The peak altitude of 174 km was reached in 220 sec. Reduction of the Nikon camera aspect data showed that the Aerobee attitude-control system oriented the rocket toward γ Cas within 0°3 in roll, 0°6 in pitch, and 1°4 in yaw and kept it steady within $\pm 20'$.

The fine-stabilization system employing a passive gyro has been described by Morton and Spitzer (1966). Imperfect performance of this stabilization system limited the useful data to an 88-sec exposure in which the spectral lines had an 8° tilt. Despite this problem, the spectrum of γ Cas from 1060 to 2130 Å was photographed with a resolution of about

* Present address: Laboratory for Atmospheric and Space Physics, University of Colorado, Boulder, Colorado 80302.

2 Å. The lower limit of 1060 Å was set by the edge of the film but is the shortest wavelength yet obtained with the Princeton all-reflective camera. The high efficiency in the far-ultraviolet was due to overcoating the mirrors and grating with a thin layer of lithium fluoride and then keeping the relative humidity below 50 percent.

a) Data Reduction

The densitometry was done by scanning the spectrum in a raster pattern with a 5- μ circular spot. A calibration curve and the intensity tracing in Figure 1 were constructed on the assumption that the Kodak 101-01 flight film had no reciprocity failure. This film

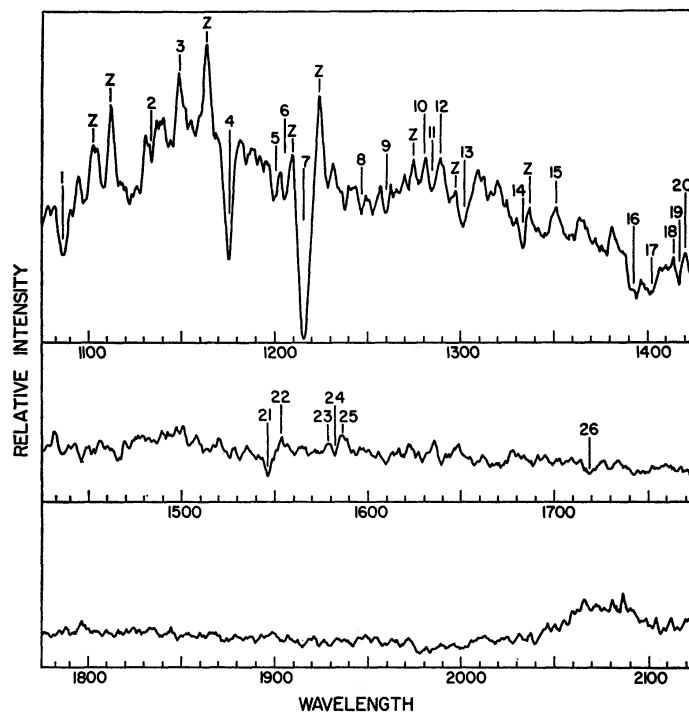


FIG. 1.—Microdensitometer tracing of the γ Cas rocket spectrogram. The abscissa is in angstroms, and the ordinate represents relative intensity without correction for the variation of instrumental sensitivity with wavelength. Features are numbered according to Table 1, except for the zero orders, which are denoted by the symbol *Z*.

had a measured dynamic range of more than 2 orders of magnitude. In comparison, Smith (1969) found a dynamic range of only a factor of 2 for Kodak Pathé SC5, another popular rocket ultraviolet film.

The zero-order star images overlying the first-order γ Cas spectrum are marked with a *Z* in Figure 1, while the real spectral features are numbered in accordance with Table 1. The intensity rise near 2050 Å is probably due to the superposition of the second-order spectrum. The lines were measured with a Gaertner engine, and the wavelengths were calculated from the grating equation by the method described by Morton *et al.* (1968) by using the position of the narrow zero-order DM+54°3025 for reference. The film scale was derived from a two-dimensional least-squares fit of the measured positions of forty zero-order images to their cataloged coordinates. A nominal wavelength accuracy of 1 Å is expected, but the uncertainty in the film scale may cause somewhat larger errors far from *La*, since the wavelength scale was determined by fitting the laboratory wavelength to the measured position of *La*. Errors in the choice of the continu-

um and the level of the background noise could change the equivalent widths in Table 1 by a factor of 2 in some cases. The laboratory wavelengths, the multiplet numbers, and the excitation potentials (E.P.) are from Moore (1950, 1965), while total oscillator strengths (gf) are taken from Wiese, Smith, and Glennon (1966), Lawrence and Savage (1966), Savage and Lawrence (1966), Gaillard and Hesser (1968), Hofmann (1969), or Wiese, Smith, and Miles (1969).

TABLE 1
ULTRAVIOLET LINES AND POSSIBLE IDENTIFICATIONS IN γ CAS

No.	λ (Obs.) (Å)*	W (Å)†	Ion	λ (Laboratory) (Å)	No.‡	E.P. (eV)	gf	Origin§
1.....	1086.7	+1.8	N II	1084.0–1085.7 (six lines)	1	0–0.02	0.98	<i>P</i>
2.....	1134.1 nw	+0.4	N I	1134.2, 1134.4, 1135.0	2	0	0.32	<i>I</i>
3.....	1148.7 ne	–0.9
4.....	1175.2 bs	+3.1	C III	1174.9–1176.4 (six lines)	4	6.5	2.3	<i>P</i>
5.....	1200.7 w	+0.9	{N I S III	{1199.6, 1200.2, 1200.7 1201.0, 1201.7, 1202.1	{1 1	{0 0.10	{1.0 3.0	{ <i>I</i> <i>P</i>
6.....	1205.9	+0.5	{Si III Si III	{1206.5 1206.5	{2 11	{0 10.3	{1.7 5.3	{ <i>P</i> <i>P</i>
7.....	1215.7 bs	+7.5	H I	1215.7	1	0	0.83	<i>I</i>
8.....	1247.2 w	+0.5	C III	1247.4	9	12.6	0.27	<i>P</i>
9.....	1260.4	+0.5	Si II	1260.4	4	0	1.1	<i>I</i>
10.....	1282.1 e	–0.3
11.....	1284.3 nw	+0.1
12.....	1290.1 w	–0.4
13.....	1300.9 bw	+2.2	{Si III O I	{1294.5–1303.3 (six lines) 1302.2	{4 2	{6.5–6.6 0	{5.1 0.25	{ <i>P</i> <i>I</i>
14.....	1334.0	+0.4	C II	1334.5	1	0	0.23	<i>I</i>
15.....	1351.0 bw	–1.2
16.....	1392.6 b	+5.6	{Si IV Si IV	{1393.8 1402.8	{1 1	{0 0	{1.1 0.53	{ <i>P</i> <i>P</i>
17.....	1402.3
18.....	1414.4 w	–0.2
19.....	1416.7	+0.5	Si III	1417.2	9	10.3	0.78	<i>P</i>
20.....	1420.0 e	–0.4
21.....	1547.2 b	+3.3	C IV	1548.2, 1550.8	1	0	0.57	<i>C</i>
22.....	1553.5 b	–0.7	C IV	1548.2, 1550.8	1	0	0.57	<i>C</i>
23.....	1580.4 ne	–0.2
24.....	1583.3	+0.3
25.....	1587.0 w	–1.0
26.....	1718.7 bw	+2.2	N IV	1718.5	7	16.1	1.14	<i>P</i>

* Character of observed line: *b*, broad; *n*, narrow; *s*, strong; *w*, weak; *e*, emission.

† Negative values of W indicate emission lines.

‡ Ultraviolet multiplet number.

§ Probable origin of line: *P*, photosphere; *C*, circumstellar shell; *I*, interstellar medium.

b) Line Identification

Six of the possible identifications in Table 1 are listed as interstellar and eleven more as stellar. The strong, broad *L* α line of hydrogen must be predominantly interstellar. The C II line with a measured wavelength of 1334.0 Å is likely to be interstellar, since the stronger 1335.7 Å component of the multiplet from the 0.01-eV level is missing. In addition, the observation of C III and C IV indicates that the state of ionization in some regions of the stellar atmosphere is too high for C II to exist in appreciable amounts. To a good approximation, the most abundant interstellar species of an element is the first ionic state to have an ionization potential greater than 13.6 eV, the value for hydrogen. Since 14.5 eV are required to ionize N I, the two resonance transitions of N I could be

interstellar while the N II 1085 Å line must be stellar. Jastrow (1965) indicates that the telluric nighttime densities of N I are too low to cause even a 0.1 Å equivalent width for the N I 1134 Å feature. Unfortunately, the stellar S III resonance multiplet at 1201 Å probably contaminates the N I 1200 Å multiplet.

Higher resolution is needed to distinguish a possible O I 1302 Å interstellar line from a broad stellar Si III multiplet (UV 4). Two other Si III multiplets that arise from the same 6.6-eV level are missing. One multiplet (UV 5) consisting of six lines from 1108 to 1113 Å is confused by a zero-order image, while the other (UV 3.05), with lines at 1447 and 1442 Å, is somewhat weaker and probably should not be expected to appear. Further evidence for Si III is the presence of the 1206 Å resonance line and the two strongest lines from 10 eV. A plausible identification for the 1260 Å feature would be Si II, since it has the largest *gf*-value of any of the Si II resonance lines. If this is the correct identification, the line must be interstellar, because the stronger companion at 1265 Å from 0.04 eV is missing. The unidentified line near 1583 Å deserves special mention, since it has appeared in spectra of ϵ Ori, ζ Ori, and ζ Pup taken with the same instrument (Morton, Jenkins, and Brooks 1969) and is the most prominent unidentified feature on the γ Cas negative.

c) Comparison with Spectra of Other Stars

In the rocket ultraviolet, spectra of moderate resolution are available for three stars with spectral types near that of γ Cas. Morton and Spitzer (1966) have obtained spectra of δ Sco (B0 V) and π Sco (B1 V) of good quality between 1260 and 1700 Å. Smith (1969) recorded the spectrum of α Vir (B1 V) from 930 to 1350 Å. Most of the weaker lines identified in δ and π Sco and α Vir cannot be seen in γ Cas. It is possible that this apparent absence is caused partly by the lower resolution of 2 Å on this flight compared with 1 Å for the Scorpius stars and 0.8 Å for α Vir, and partly by excessive fogging, which reduced the contrast of the lines on the film. In addition, the rotational velocity $v \sin i = 300 \text{ km sec}^{-1}$ for γ Cas (Boyarchuk and Kopylov 1964) is about a factor of 2 greater than for the other three stars, so that the γ Cas lines will be intrinsically about 1 Å wider. The only obvious difference between γ Cas and the main-sequence Scorpius stars is the C IV emission near 1550 Å.

The C IV line has a P Cygni profile similar to that observed in three Orion supergiants and ζ Pup by Morton *et al.* (1968, 1969), but the absorption component in γ Cas has a velocity shift of only -450 km sec^{-1} toward the observer, which is much less than the typical values of -1200 to $-1800 \text{ km sec}^{-1}$ summarized by Morton (1969*a*) for stars of greater luminosity. Normally, the emission part of a P Cygni profile lies closer to the laboratory wavelength than the absorption component. Thus, the measured shift of $+780 \text{ km sec}^{-1}$ for the emission relative to only -450 km sec^{-1} for the absorption in γ Cas may be due to an unexpectedly large wavelength error that exceeds 1 Å at 1550 Å, so that the absorption could be shifted by -700 km sec^{-1} or more. Although P Cygni profiles for Si IV and shifted absorption for Si III, N V, and C III were found in the Orion supergiants, no similar effects are observed for these lines in γ Cas. Certainly, more high-resolution observations of γ Cas and of other Be stars are needed in the ultraviolet to determine more accurately any possible wavelength shifts.

III. OAO ULTRAVIOLET SPECTRUM

To complement the Princeton University Observatory (PUO) rocket data, several scans of γ Cas obtained by the first successful OAO have been supplied by T. Houck of the Washburn Observatory of the University of Wisconsin. Four tracings, each representing the average of at least two OAO scans, are shown in Figures 2 and 3. The data were obtained in 1969 July and August and cover the wavelength region 1100–4000 Å. To facilitate comparison with the OAO scans, the PUO spectra of γ Cas and of three Orion stars (Morton *et al.* 1968) were renormalized so that the continuum would be

similar to that of the short-wavelength OAO spectrum, while the rocket resolution was degraded by convolution with the OAO slit profile, which was about 16 \AA wide at half-maximum. The zero-order images in the γ Cas spectrum were removed before convolution.

a) Equivalent Widths

Equivalent widths of the stronger lines in γ Cas derived from the OAO and PUO data are compared in Table 2. At the OAO resolution, the 1201 and 1206 \AA lines are blended with $L\alpha$, increasing the apparent $L\alpha$ equivalent width by 1.4 \AA to a total of 8.9 \AA , a value which is in remarkable agreement with the OAO result. In general, problems of line blending and the position of the continuum become worse at lower resolution; therefore,

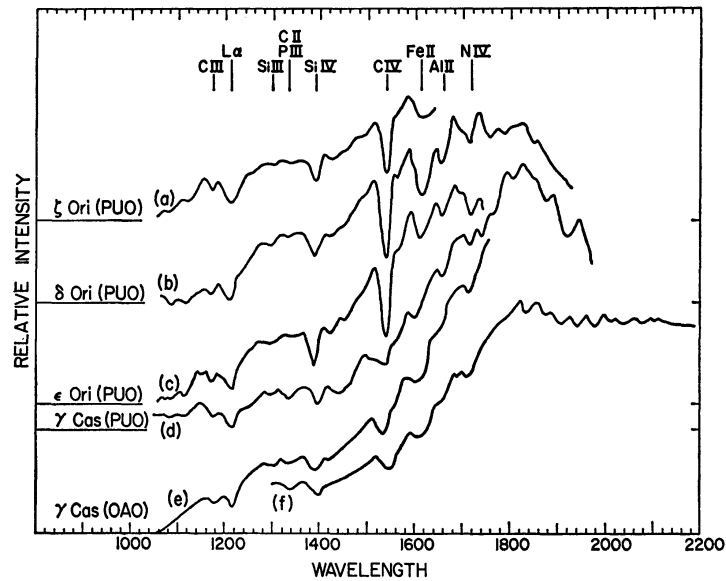


FIG 2. — Degraded rocket spectra of (a) z Ori (09.5 Ib), (b) δ Ori (09.5 II), (c) ϵ Ori (B0 Ia), and (d) γ Cas (B0.5 IVpe) compared with two OAO scans of (e) and (f) γ Cas. Zero level for each scan is indicated by the horizontal line below the star name. No corrections have been made for instrumental sensitivity, but the rocket spectra have been normalized to the OAO scans.

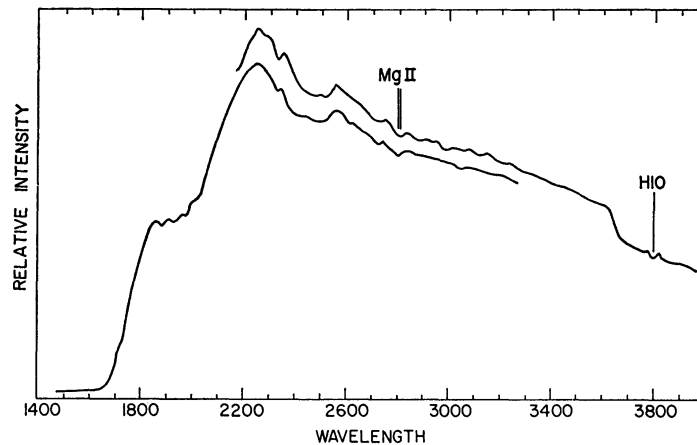


FIG. 3.—Two OAO scans of γ Cas at longer wavelengths, without correction for instrumental sensitivity

the PUO values are to be preferred. However, the low PUO signal strength at C IV means that the error in the level of the background noise will cause a large uncertainty in the equivalent width, so that the OAO C IV value probably should be given more weight.

The OAO feature identified as C II in Table 2 in fact must be a blend of lines. Not only is the equivalent width more than 5 times that derived from the rocket data, but the wings are wider than would be expected if C II were the only contributor. The most likely candidate for broadening the absorption is stellar P III (UV 1), with components at 1335 Å ($gf = 1.3$) and 1344 Å ($gf = 2.5$). The 1344 Å component from 0.07 eV cannot be visually identified on the γ Cas rocket spectrogram, although it may be a major contributor to the very broad feature near the correct wavelength in Figure 1. In the high-resolution Orion spectra, the 1344 Å line is identified in all three stars.

b) Line Identification

Further identifications for features in the γ Cas OAO scans are suggested by the Orion data. Although the spectral types of δ Ori (O9.5 II), ϵ Ori (B0 Ia), and ζ Ori (O9.5 Ib) differ somewhat from the B0.5 IVpe designation for γ Cas, the OAO scans presented by Code and Bless (1970) show continuity in the strengths of many of the features present from B0.5 to O9.5 for main-sequence stars and supergiants. Furthermore, at the low

TABLE 2
EQUIVALENT WIDTHS FOR FEATURES IN γ CAS (IN Å)

	C III 1176 Å	La 1216 Å	Si III 1300 Å	C II 1334 Å	Si IV 1397 Å	C IV 1549 Å	N IV 1718 Å
PUO (rocket) . . .	3.1	8.9*	2.2	0.4	5.6	2.6†	2.2
Wisconsin (OAO)	3.7	9.0	1.2	2.2	4.7	5.5	1.6

* Includes 1.4 Å from the blended features at 1201 and 1206 Å.

† Net value for absorption and emission components.

resolution of the OAO, there are no striking differences between γ Cas and main-sequence stars with types near B0.5. Therefore, at the longer wavelengths where the γ Cas rocket signal strength is low, we assume that corresponding features in the PUO Orion data and the OAO γ Cas data are likely to be caused by the same ion.

The broad absorption centered near 1615 Å in the OAO spectrum of γ Cas probably arises almost entirely from the UV 8 multiplet of Fe II. Neither the strong C III line at 1591 Å in ϵ and ζ Ori nor the He II line at 1640 Å contributes significantly to the corresponding feature in these stars. The slight dip at 1660 Å in γ Cas is persistently present in the OAO data for stellar types hotter than B0.5 and reaches maximum intensity in the O9.5 supergiants in correlation with the rocket data. In ϵ and δ Ori, this feature is primarily a blend of two lines measured near 1657 and 1672 Å. The first line also appears in ζ Ori, but the long-wavelength cutoff of 1670 Å precludes confirmation of the second. Identification of the latter line as the ultimate line of Al II is plausible, but it seems unreasonable for the former to be C I in such hot stars. Both lines have much too great an equivalent width to be entirely interstellar. Finally, the absorption near 1720 Å present in all the stars shown in Figure 2 is probably a blend of N IV and an unidentified feature at 1724 Å which contributes 30–40 percent of the absorption in δ and ϵ Ori.

There are fewer readily identifiable features on the long-wavelength OAO scan in Figure 3. The resonance doublet of Mg II at 2800 Å is probably present. Henize, Wray, and Wackerling (1968) observed this line in several spectra of B stars photographed by *Gemini XI* and *XII* astronauts. Comparison of Figures 3 and 4 indicates that the dip at 3800 Å on the OAO scan is most likely H10.

IV. VISUAL SPECTRUM

A visual spectrogram of γ Cas from 3500 to 5000 Å with a dispersion of 12 Å mm⁻¹ has been provided by John F. Heard and Frederick R. Hickok of the David Dunlap Observatory. The visual spectrum was taken 1968 November 18 at 23^h55^m U.T., less than 4 days after the rocket flight that secured the ultraviolet spectrum.

The γ Cas visual spectrum, the iron-line comparison spectra, and calibration wedge were scanned with a digital densitometer with a slit 4 × 585 μ. Only those lines for which the central intensity dropped by about 0.2 units below the continuum on the relative intensity scale of Figure 4 were chosen for inclusion in Table 3. Wavelengths are

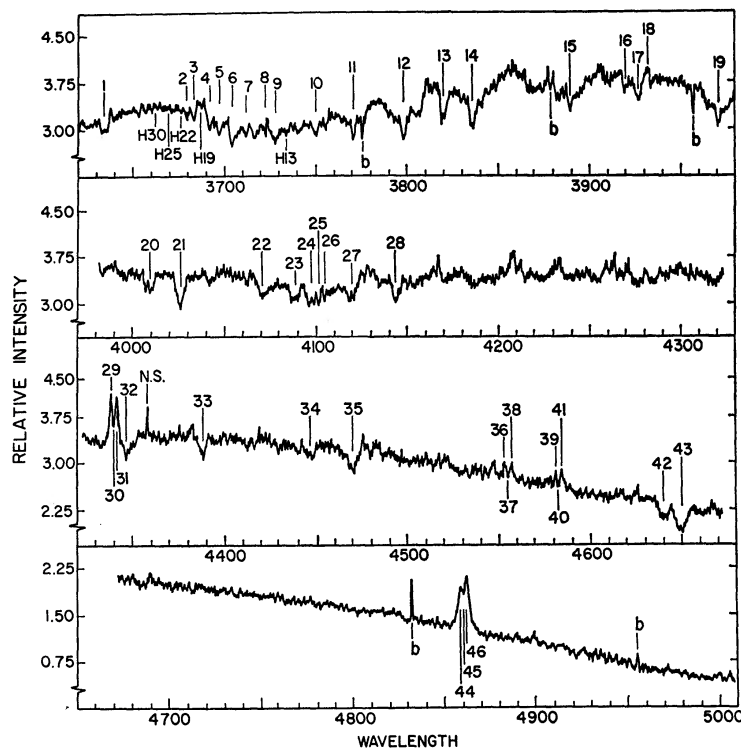


FIG. 4.—Microdensitometer tracing of the visual γ Cas spectrum. Features are numbered according to Table 3. Film blemishes are marked on tracing with the letter *b*, while *N.S.* indicates the night-sky 4358 Å Hg γ line. Numbers on the ordinate show the relative intensities above zero.

accurate to 0.1 Å for narrow lines but are less certain for broad, asymmetric profiles. The wavelengths have been corrected for the -16 km sec⁻¹ orbital and rotational motion of the Earth and the -7 km sec⁻¹ radial velocity of γ Cas given by Wilson (1953). The multiplet numbers and excitation potentials are from Moore (1945).

The observed Balmer sequence runs from H β to H21. Double peaked emission at H β and H γ rises 60 and 20 percent, respectively, above the continuum. The remainder of the series consists of absorption lines increasing in strength to a maximum at H9 and then generally decreasing thereafter. Near H13, the Balmer lines are anomalously weak. The positions of lines lacking the minimum strength needed for inclusion in Table 3 are identified in Figure 4. The relatively small amount of absorption at H δ is undoubtedly due to a filling in by line emission caused by the same process that produces emission at H α , H β , and H γ . H ϵ and probably H8 through H11 exhibit broad, shallow dish-shaped profiles with wings 20 to 30 Å wide. These Stark-broadened photospheric profiles have the

TABLE 3
VISUAL LINES AND POSSIBLE IDENTIFICATIONS IN γ CAS

No.	λ (Obs.) (Å)*	Ion†	λ (Laboratory) (Å)	No.‡	E.P. (eV)	<i>gf</i>
1.....	3634.3	He I	3634.2	28	20.9	0.078
2.....	3679.4	H21	3679.4	4	10.2	0.00304
3.....	3683.3	H20	3682.8	4	10.2	0.00353
4.....	3692.0	H18	3691.6	4	10.2	0.00488
5.....	3697.5	H17	3697.2	3	10.2	0.00582
6.....	3704.0	{H16 He I	{3703.8 3705.0	{3 25	{10.2 20.9	{0.00701 0.14
7.....	3711.9	{H15 O II	{3712.0 3712.8	{3 3	{10.2 22.9	{0.00856 0.23
8.....	3722.7	H14	3721.9	3	10.2	0.0106
9.....	3728.2	O II	3727.3	3	22.9	0.49
10.....	3750.1	{H12 O II	{3750.2 3749.5	{2 3	{10.2 22.9	{0.0172 0.76
11.....	3770.7	H11	3770.6	2	10.2	0.0227
12.....	3798.1	H10	3797.9	2	10.2	0.0308
13.....	3820.0	He I	3819.6	22	20.9	0.19
14.....	3835.9	H9	3835.4	2	10.2	0.0434
15.....	3889.5	{H8 He I	{3889.1 3888.6	{2 2	{10.2 19.7	{0.0643 0.19
16.....	3920.1	C II:	3920.7, 3919.0	4	16.3	0.57, 0.29
17.....	3926.9	He I	3926.5	58	21.1	0.022
18.....	3933.9	Ca II:	3933.7	1	0	1.4
19.....	3970.1	He I	3970.1	1	10.2	0.102
20.....	4009.5	He I	4009.3	55	21.1	0.034
21.....	4026.2	He I	4026.2	18	20.9	0.43
22.....	4071.2	O II	{4075.9, 4072.2, 4069.9, 4069.6}	10	25.5	{5.0, 3.4, 2.2, 1.4
23.....	4088.7	Si IV	4088.9	1	24.0	1.6
24.....	4097.8	N III	4097.3	1	27.3	0.97
25.....	4101.9	H δ	4101.7	1	10.2	0.177
26.....	4105.1	O II	4104.7, 4105.0	20	25.7	1.6, 0.81
27.....	4120.0	O II	{4119.2, 4120.3, 4120.6}	20	25.7	{3.0, 0.68, 0.075
28.....	4143.7	He I	4143.8	53	21.1	0.064
29.....	4339.1e}	H γ	4340.5	1	10.2	0.357
30.....	4340.6					
31.....	4342.3e}					
32.....	4347.3	O II	{4349.4, 4345.6 4351.3, 4347.4	{2 16	{22.9 25.6	{1.3, 0.50 1.6, 1.1
33.....	4389.2	He I	4387.9	51	21.1	0.13
34.....	4447.8	N II:	4447.0	15	20.3	1.9
35.....	4471.3	{He I He I	{4471.5 [4469.9]	{14 15	{20.9 20.9	{1.1 ...
36.....	4554.0e}	Fe II	4555.9	37	2.82	...
37.....	4555.8					
38.....	4557.8e}					
39.....	4582.2e}	Fe II	4583.8	38	2.79	...
40.....	4583.6					
41.....	4585.4e}					
42.....	4641.1	{N III O II	{4640.6, 4641.9 4641.8, 4638.9	{2 1	{30.3 22.9	{... 1.5, 0.54
43.....	4650.5	{O II C III	{4649.1, 4650.8 4647.4, 4650.2, 4651.4	{1 1 ...	{22.9 29.4 ...	{2.7, 0.53 1.3, 0.76, 0.25
44.....	4859.8e}	H β	4861.3	1	10.2	0.954
45.....	4861.6					
46.....	4862.9e}					

* e=emission line.

† Colon indicates identification less certain.

‡ Visual multiplet number.

narrower absorption lines of the envelope superimposed. Shortward of H16, Balmer continuous emission is detectable.

Most of the expected He I lines are present with broad photospheric absorption profiles. The strength of the 4713 Å line relative to the other He I lines seems to be too weak for a gf -value of 0.11, while the 3926 Å feature is perhaps too deep in comparison with the other lines.

Evidence for heavier elements in the visual spectrum of γ Cas is not quite as conclusive. Identification of the feature at 3920 Å as C II is very uncertain, because the stronger doublet at 4267 Å is missing and the ultraviolet spectrum indicates that C II may be interstellar. Absorption by a C III triplet undoubtedly contributes to the broad feature at 4650 Å, since this triplet reaches maximum intensity near type B0 according to Merrill (1956).

Emission profiles similar to those of H β and H γ are present at 4556 and 4584 Å. These features are probably produced by two of the strongest Fe II emission lines recorded by Baldwin (1942) during the great outburst of 1937. These same two emission lines can be identified on most of the spectra presented by Cowley and Marlborough (1968) in their photographic history of γ Cas.

In summary, only hydrogen and helium are present with absolute certainty. However, the remainder of the identifications seem quite likely, except for those marked with colons in Table 3.

V. INTERSTELLAR OBSERVATIONS

a) Neutral Hydrogen

The measured equivalent width of the L α interstellar-hydrogen absorption line is $W = 7.5 (+3, -1.5)$ Å. Misplacement of the continuum or an error in compensating for the zero-order images that lie on either side of L α is the primary cause for the quoted possible errors of +3 and -1.5 Å. The neutral-hydrogen column density $N(\text{H I})$ to γ Cas calculated on the assumption that the broad wings are caused by radiation damping alone gives

$$N(\text{H I}) = 1.865 \times 10^{18} W^2 = 1.0 \times 10^{20} \text{ cm}^{-2}.$$

A small amount of high-velocity neutral hydrogen between the Sun and γ Cas could invalidate the radiation-damping hypothesis. However, for an exponential distribution of gas, a dispersion η (see eq. [1] below) of over 80 km sec $^{-1}$ would be necessary to reduce $N(\text{H I})$ significantly. This dispersion is about 10 times that usually found from optical and 21-cm radio data (Spitzer 1968), although there could be a secondary component of the interstellar medium with a weak tail at very high velocities.

The spectroscopic distance to γ Cas can be calculated from the visual magnitude of 2.2, the spectral type of B0.5 IV of Morgan (Osterbrock 1957), and the absolute visual magnitude of -4.45 interpolated from the data of Blaauw (1963). Interstellar reddening and Paschen emission by the envelope introduce uncertainties on the order of 30 pc, but the two effects tend to cancel each other. We adopt a distance of 220 pc and obtain an average H I density of $n(\text{H I}) = 0.15$ atoms cm $^{-3}$. Jenkins (1970) has discussed the differences between the rocket ultraviolet densities and the 21-cm radio data which give typical densities of 0.7 atoms cm $^{-3}$ (Kerr and Westerhout 1965) in the solar neighborhood.

b) Other Elements

The lines of N I at 1134 Å, Si II at 1260 Å, and C II at 1334 Å are the most likely additional candidates for uncontaminated interstellar absorption in the spectrum of γ Cas. If the velocity distribution of the interstellar gas is Maxwellian with a dispersion σ less than 25 km sec $^{-1}$, all three lines will be broadened by the damping wings of their natural, Lorentzian absorption profiles. However, column densities N calculated on this basis indicate that the interstellar N I, C II, and Si II would be unreasonably overabundant relative to hydrogen as shown in Table 4 under the description "nat."

As noted by Stone and Morton (1967), if the interstellar medium contains enough gas at radial velocities where the wings of the saturated lines are formed, Doppler broadening will dominate and the derived densities will be much less. For example, an exponential velocity distribution of gas of the form

$$\phi(v) = \frac{1}{2^{1/2}\eta} \exp\left(-\frac{2^{1/2}|v|}{\eta}\right) \quad (1)$$

with $\eta = 15 \text{ km sec}^{-1}$ gives the column densities N in Table 4. Similarly, column densities for the interstellar lines found in δ and π Sco by Stone and Morton (1967) are also recomputed and included in the table. The final rows of Table 4 are the quotients of N to the star divided by the expected abundances of each element for the cases of (1) an

TABLE 4
EQUIVALENT WIDTHS, COLUMN DENSITIES, AND SOLAR RATIOS
FOR POSSIBLE INTERSTELLAR LINES

	ION					
	C II	N I	O I	Si II	Si II	Al II
λ (Å)	1334.5	1134	1302.2	1260.4	1526.7	1670.8
f	0.11	0.08	0.05	0.57	0.13	1.8
W (Å):						
γ Cas	0.44	0.42	...	0.46
δ Sco	0.9	...	1.2	...	0.6	1.2
π Sco	0.9	...	1.1	...	0.45	...
N (cm^{-2}) for exp.:						
γ Cas	3.1×10^{15}	10^{15*}	...	1.1×10^{15}
δ Sco	4.1×10^{17}	...	3.2×10^{19}	...	6.0×10^{15}	3.8×10^{16}
π Sco	4.1×10^{17}	...	1.1×10^{19}	...	1.5×10^{15}	...
N/N_{solar} :						
γ Cas exp.	0.06	0.1	...	0.33
γ Cas nat.	41	400†	...	33
δ Sco exp.	0.65	...	29	...	0.16	20
δ Sco nat.	15	...	17	...	13	3 ζ
π Sco exp.	1.0	...	16	...	0.06	...
π Sco nat.	24	...	22	...	12	...

* Because the N I 1134 Å multiplet consists of three overlapping lines all from zero excitation potential, the column density was estimated from a detailed construction of the absorption profile of the multiplet and not from eq. (3).

† The value of 400 is a lower limit obtained by assuming the damping wings of the three components of the multiplet do not significantly overlap.

exponential velocity profile ("exp.") with $\eta = 15 \text{ km sec}^{-1}$ and (2) natural line broadening ("nat."). The expected abundances are computed from the column densities of H I to γ Cas and to the Scorpius stars (Jenkins, Morton, and Matilsky 1969) by assuming that the observed ion is the dominant species and using the solar ratios for each element found by Goldberg, Müller, and Aller (1960).

An exponential velocity distribution with a dispersion as large as $\eta = 15 \text{ km sec}^{-1}$ for the bulk of the neutral hydrogen probably cannot be reconciled in detail with the 21-cm data of Westerhout (1969) in the direction of γ Cas. It is possible, however, that the ultraviolet absorption lines could arise from a tenuous intercloud medium with a large velocity dispersion which might not register on the 21-cm profiles.

For interstellar Na I and Ca II lines, Münch (1968) finds that an exponential velocity distribution with $\eta = 4.7 \text{ km sec}^{-1}$ for Na I and $\eta = 8.5 \text{ km sec}^{-1}$ for Ca II best describes the data for nearby stars. Perhaps the exponential wings of the interstellar species considered in this paper are formed in either a tenuous intercloud medium or in high-velocity clouds where the sodium and calcium are primarily Na II and Ca III. Münch

(1968) also gives the curve of growth for an exponential absorption profile. For large central optical depths ($\tau_0 \gtrsim 10$), the asymptotic result is

$$W = .2^{1/2}(\lambda_0\eta/c) \ln (1.78\tau_0) . \quad (2)$$

For the dispersion $\eta = 15 \text{ km sec}^{-1}$, the column density to the star is

$$N = \frac{4.50 \times 10^{16}}{f\lambda_0} \exp (1.41 \times 10^4 W/\lambda_0) \text{ cm}^{-2} , \quad (3)$$

where W and λ_0 are in angstroms.

Only in two cases do the ratios for natural broadening agree better with solar abundance ratios than do the "exp." values. However, the exponential term in equation (3) makes the column densities much more sensitive to experimental errors in the equivalent widths. If we are observing the predominant ionic species in each case, then an exponential velocity distribution with $\eta = 15 \text{ km sec}^{-1}$ yields column densities which agree with the solar ratios within the experimental error of every measured equivalent width. For example, the worst disparities for C II in γ Cas and for Si II in π Sco require less than a 70 percent increase in W to obtain agreement with the expected abundances. In contrast, W must be reduced by more than a factor of 3 to achieve the same result, if the lines are formed by radiation damping.

Caution is required when equation (3) is applied, because it is valid only when the exponential broadening for $\eta = 15 \text{ km sec}^{-1}$ dominates over radiation damping. For example, the misapplication of equation (3) to the broad L α lines or to the O I line in δ Sco results in column densities which are larger than those calculated for natural broadening. However, re-examination of the original Scorpius plate indicates that there may be some broadening of the O I lines caused by the stellar Si III multiplet. Only a 25 percent allowance for contamination in the case of δ Sco is necessary to bring the "exp." ratio for O I in Table 4 down to unity.

c) Molecular Hydrogen

The absence of any detectable lines of molecular hydrogen allows the determination of an upper limit on the mean density of interstellar H₂ to γ Cas. Spitzer, Dressler, and Upson (1964) show that for temperatures less than about 30° K, essentially all of the molecules will be in the ground rotational level ($J = 0$). For broadening by radiation damping alone, a line of the minimum observable equivalent width ($W = 0.2 \text{ \AA}$) at 1077 \AA corresponds to a maximum column density of $N(\text{H}_2) = 1.7 \times 10^{18} \text{ cm}^{-2}$. This is about 2.4×10^{-3} hydrogen molecules per cubic centimeter and can be compared with the results of Smith (1969), who finds $n(\text{H}_2) < 6 \times 10^{-4} \text{ cm}^{-3}$ in the direction of α Vir. The f -values of Dalgarno and Allison (1968) have been used to compute these upper limits on the interstellar H₂.

If a 1077 \AA line of H₂ with $W = 0.2 \text{ \AA}$ were formed by a Gaussian velocity distribution of cold clouds with an external velocity dispersion greater than 8 km sec⁻¹, the line would lie on the Doppler or linear part of the curve of growth. In this case, the upper limit would correspond to a value of $n(\text{H}_2)$ even smaller than $2.4 \times 10^{-3} \text{ cm}^{-3}$.

VI. PROPERTIES OF THE STELLAR ENVELOPE

a) Electron Density

According to Griem (1964), Balmer continues emission, which is observed in γ Cas, advances down to the position of that Balmer line whose Stark-broadened width is equal to its separation from the next line in the series. Griem gives a modified Inglis-Teller formula that relates the electron density n_e to the quantum number n of the last observed line or, equivalently, the line to which continuous emission extends,

$$\log n_e = 22.6 - 7.50 \log n . \quad (4)$$

The Balmer continuous emission begins to rise near the H16 absorption line, which indicates that significant emission occurs at electron densities as great as $4 \times 10^{13} \text{ cm}^{-3}$, while the highest hydrogen absorption line at $n = 21$ means that there is little Balmer absorption at n_e less than about $5 \times 10^{12} \text{ cm}^{-3}$.

b) *Balmer Discontinuity*

The Balmer discontinuity obtained from the OAO data is

$$D = \log L(\lambda 3647+) / L(\lambda 3647-) = -0.08 .$$

For a normal B0.5 V star, Aller (1963) gives $D = +0.09$, so that the luminosity of the Balmer continuous emission of the envelope is about 0.4 times the luminosity of the star $L_*(\lambda 3647+)$ measured far enough longward of the Balmer jump to exclude the advanced Balmer continuous emission. The value of 0.4 depends slightly on the amount of envelope emission present at $3647+ \text{ \AA}$ (see eq. [6]), but the value will be only 0.5, even if the envelope emits as much as 30 to 75 percent as much light as the star at $3647+ \text{ \AA}$. On the other hand, the factor of 0.4 will have to be reduced accordingly if the envelope were to absorb a significant fraction of the photospheric light at $3647+ \text{ \AA}$. If the entire envelope is optically thin in the Balmer continuum, a volume-temperature relation and the amount of emission longward of the Balmer jump can be deduced directly.

i) *Volume of Envelope*

The model atmosphere of Van Citters and Morton (1970) for a B0.5 V star with an effective temperature T_{eff} of 25200° K and bolometric correction of -2.51 is used to approximate the photospheric distribution of spectral-energy flux in γ Cas. The absolute visual magnitude of -4.45 (Blaauw 1963), together with the model parameters, determines the radius $R_* = 11 R_\odot$ and the luminosity at the Balmer jump as well as the mass $M_* = 20 M_\odot$ from model interiors by Stothers (1963) and Iben (1966). Ambartsumyan (1958) gives the theoretical distribution of energy for an electron-proton recombination spectrum. Setting the observed continuous Balmer emission $0.4 L_*(\lambda 3647+)$ equal to the theoretical value determines the effective emitting volume V_E of an optically thin envelope if the electron temperature T is known:

$$V_E / V_* = 3.1 \times 10^{30} T^{3/2} R_*^{-1} n_e^{-2} , \quad (5)$$

where V_* is the volume occupied by the star. Large temperature gradients are probably present in the emitting region. However, a typical temperature of nearly 20000° K seems to be necessary to explain the line veiling as discussed in the next paragraph. Since the effective photospheric temperature is about 25200° K , a somewhat lower isothermal electron temperature of $T = 20000^\circ \text{ K}$ for the envelope may be reasonable and will be adopted for the purposes of the following discussions. For the typical electron density of about 10^{13} cm^{-3} found from the Inglis-Teller relation, the volume of an optically thin emitting region from equation (5) is $V_E = 0.1 V_*$. This value should be regarded as a lower limit, because any emitting gas hidden behind the star or any nonzero optical depth at the head of the Balmer continuum implies an emitting volume greater than $0.1 V_*$ in order to produce the observed amount of Balmer emission.

ii) *Visual Line Veiling*

Accompanying the Balmer continuous emission are recombination spectra of the Paschen and higher continua, which will cause a veiling or apparent decrease in the strengths of the visual photospheric lines. For an optically thin envelope at $T = 20000^\circ \text{ K}$, the luminosity between the series limits of 3647 and 8206 \AA is

$$L_E(\nu) = 0.67 L_*(\lambda 3647+) \exp(-h\nu/kT) \text{ ergs sec}^{-1} \text{ Hz}^{-1} , \quad (6)$$

found by summing the emission coefficients for the free-free, Paschen, and higher hydrogen bound-free continua according to Ambartsumyan (1958). Again, with the 25200° K model atmosphere of Van Citters and Morton for the underlying stellar continuum, equation (6) implies that photospheric equivalent widths will be reduced by 35, 16, and 20 percent at 3500, 4500, and 5000 Å, respectively, due to the overlying emission from an optically thin envelope at 20000° K. The numerical coefficient in the Balmer continuum is 3.5 instead of the 0.67 in equation (6). The amount of veiling decreases sharply for an electron temperature below 20000° K, but increases only moderately for higher temperatures. For example, only a 5 percent reduction in equivalent widths at 4500 Å will result for 10000° K, while the reduction would be 24 percent for a temperature as high as 30000° K. There will be little veiling in the far-ultraviolet, as the emission is less than 2 percent of the star's luminosity at 1500 Å, even for an envelope at 30000° K.

Average values for two He I lines at 4388 and 4471 Å in 115 O9 to B1 stars given by Deeming and Walker (1967) indicate that these lines are about 20 to 30 percent too weak in γ Cas. Thus, somewhat more veiling of the visual lines than that calculated for the optically thin case may be present. If the optical depth $\tau(\lambda 3647-)$ for a typical line of sight through the emitting regions is not small, the Balmer emission will be self-absorbed, and therefore more emission than calculated above will emerge in the tails of the hydrogen continua. A typical optical depth $\tau(\lambda 3647-)$ of only unity could approximately double the calculated veiling longward of 3647 Å.

iii) *Projected Area of Envelope*

Now consider the more general case where $\tau(\lambda 3647-)$ in the envelope is not arbitrarily restricted, so that the specific intensity emitted by an isothermal envelope is $(1 - \exp[-\tau_\lambda])$ times the Planck blackbody function $B(\lambda, T)$. Consequently, the measured Balmer discontinuity means that the emission intensity at 3647- Å integrated over the projected visible surface area of the envelope is 0.4 times the same integral at 3647+ Å for that part of the stellar photosphere not occulted by a possibly opaque envelope. If we ignore limb darkening and approximate the photospheric flux by the Planck function,

$$A_E/A_* = 0.4 B(\lambda 3647+, 25200) / \{B(\lambda 3647-, 20000)[1 - e^{-\tau(\lambda 3647-)}]\}, \quad (7)$$

where the envelope is at 20000° K with a projected area A_E relative to the unocculted photospheric area A_* at 25200° K. Of course, the envelope is not optically deep everywhere or there could be no observed Balmer continuous emission, so that equation (7) gives a firm lower limit of $A_E > 0.7 A_*$. In the following subsections, we continue to explore the observational limitations on the geometry of the envelope and then summarize and discuss them as a whole.

c) *Line Profiles*

The line emission that fills in the lower Balmer lines seems to be absent for the envelope lines higher than H9. The equivalent widths of the narrow cores of H9 to H14 (H13 excepted) decrease in proportion to their f -values, which may imply that the optical depth of the region emitting the Balmer continuum is nearly zero along the line of sight to the visible photosphere. On the other hand, the strengths of H17 through H21 (H19 excepted) are about a factor of 5 too large to be formed by absorption of the same continuum as H9 to H14. Instead, the Balmer lines shortward of H16 must be formed by self-absorption of the Balmer continuous radiation produced primarily in emission lobes off the disk of the star, which is consistent with the theory of Burbidge and Burbidge (1955) that the narrow central reversals of H β and H γ are formed by self-absorption outside the line-emission region.

For the optically thin case, the above factor of 5, together with the measurement of a

Balmer emission continuum equal to 0.4 of the stellar continuum, means that the envelope must cover less than 10 percent of the photosphere. Furthermore, a localized envelope is consistent with the observed P Cygni profile of the C iv line at 1550 Å. This resonance line must be formed outside the regions producing the Balmer lines, since they have radial velocities less than 50 km sec⁻¹, whereas the C iv absorption component may be near the escape velocity of 850 km sec⁻¹. With most of the photosphere unobscured by the envelope, the necessary radiation will be available to produce the C iv P Cygni line by the method suggested by Lucy and Solomon (1970). They propose that the ionization equilibrium is determined by the stellar radiation field, while absorption of photons in the ultraviolet resonance lines produces a negative effective surface gravity. With an effective temperature T_{eff} of 26200° K given by Morton (1969*b*), C iv will provide the main acceleration mechanism. In fact, with $\log T_{\text{eff}} = 4.42$ and the reduced surface gravity due to the high rotational velocity, γ Cas should be a prime candidate for mass loss by the instability described by Lucy and Solomon.

d) Emission-Region Models

Marlborough (1969*a, b*) has constructed a detailed model envelope supported by stellar rotation; he obtained Balmer line profiles remarkably similar to those of a star in a shell phase with deep, sharp central absorption cores for the lower emission lines and strong absorption lines as high as H35. Presently, however, γ Cas is quiescent and does not possess this type of shell spectrum. Perhaps the current line profiles of γ Cas could be reproduced by merely decreasing the extent of the wedge-shaped envelope used by Marlborough.

Even for an envelope temperature as low as the 10000° K used by Marlborough, the observed Balmer continuum emission from γ Cas may be more difficult to account for than the line profiles on the basis of Marlborough's model where continuum radiative-energy losses are balanced only by absorption of photospheric radiation. If an envelope at the electron temperature of 10000° K absorbed as much as 10 percent of the stellar flux shortward of 912 Å and converted each photon to a Balmer continuum photon, then the B0.5 model of Van Citters and Morton (1970) would be deficient by more than a factor of 100 in the ultraviolet flux required to explain the amount of emission observed in γ Cas.

An additional energy source is suggested by the work of Underhill (1949), who found that a density inversion may occur if the surface gravity is less than the outward force exerted by the radiation field. The resulting instability has been discussed by Miħalas (1969) and termed "normal convection" by Wentzel (1970). Underhill thought that the instability could cause a streaming of hot gas from the surface and that this activity might resemble the prominence action of the Sun. In any case, the high rotational velocity of γ Cas will lower the equatorial surface gravity, which would thus enhance the possibility for hot masses of gas to carry thermal and mechanical energy up from an equatorial band. Whether this gas billows up in long streamers or in discrete clouds, it will tend to wrap around the equatorial region and form a disk or ringlike structure as suggested by Edwards (1956).

On the basis of this model, a shell phase can be explained as a period of enhanced ejection activity followed by an interval during which shell absorption lines are formed by an increased amount of residual gas in the envelope, which may obscure the entire photosphere. Strongly supporting this type of model are the line profiles and continuum energy distributions exhibited by γ Cas during the period 1937–1940, as discussed by Swings and Struve (1941), Baldwin (1942), Gorbatsky (1949), and Edwards (1956).

If the envelope is being replenished by only a few hot surface elements at any given time, we might expect subtle periodic variations in the spectrum as γ Cas rotated. In fact, Hutchings (1970) has found a period of 0.7 days for γ Cas from just such a study and has independently concluded that short-lived condensations rise from the equatorial region and dissipate into an extended envelope.

To interpret the spectroscopic data in terms of a detailed model, the inclination i of the axis of rotation must be determined. Hutchings (1970) derives $i = 55^\circ \pm 10^\circ$ by fitting line profiles computed for a model envelope to the observed profiles but finds a radius for γ Cas of only $7 R_\odot$. On the other hand, the rotational period of $0^d.7$ and the radius of $11 R_\odot$ previously calculated yield an equatorial rotational velocity of 800 km sec^{-1} , unreasonably in excess of the breakup velocity of 600 km sec^{-1} . If Hutchings's period were low by a factor of 2 and if the value of Boyarchuk and Kopylov (1964) for $v \sin i = 300 \text{ km sec}^{-1}$ is increased by 40 percent as suggested by Hardorp and Strittmatter (1968), then $\sin i$ is near unity for $R_* = 11 R_\odot$. Since the 300 km sec^{-1} is among the highest values found by Boyarchuk and Kopylov, we shall assume that γ Cas has a rotational axis nearly perpendicular to our line of sight ($i \sim 90^\circ$) to simplify the discussion.

The restrictions on the geometry of an equatorial envelope at 20000° K with an electron density of 10^{13} cm^{-3} are summarized below:

1. $V_E \geq 0.1 V_*$ or $V_E = 0.1 V_*$ for $\tau(\lambda 3647-) \ll 1$.

2. $A_E = 0.7 A_*/\{1 - \exp[-\tau(\lambda 3647-)]\}$.

3. Area of photosphere covered by an optically thin envelope $< 0.1 A_*$.

For the intermediate case of $\tau(\lambda 3647-) = 1$, V_E is roughly $0.2 V_*$ and $A_E = 1.1 A_*$, where A_* now will be the entire area of the stellar disk. Condition 3 requires that most of the projected area of the envelope lie off the disk, so that any axially symmetric, continuous distribution of matter would occupy more volume than $0.2 V_*$. Thus, the most likely picture for fairly small optical depths is one where the individual radiating clouds or streamers which rise from the surface remain intact over a distance of several radii. If the envelope of γ Cas were to consist of spherical clouds of equal size, then the given volume of $0.2 V_*$ and area of $1.1 A_*$ require that there be about thirty clouds each with a radius of $0.2 R_*$. If only one or two clouds lie in the line of sight to the photosphere, condition 3 will be fulfilled.

If the typical continuum optical depth in the envelope is much greater than unity, contrary to the above example, many other geometries may be possible, including a continuous distribution of emitting matter. Observation of the Paschen discontinuity and comparison with the amount of Balmer continuous emission should settle the question of optical depth. The population of the $n = 3$ level of hydrogen will be less than the $n = 2$ level, so that a relative excess of Paschen to Balmer continuous emission over that predicted by the relative recombination coefficients will indicate that there is self-absorption in the Balmer continuum. Even if the case of $\tau(\lambda 3647-) \leq 1$ proves tenable, the equations of radiative transfer will have to be solved for the discrete-cloud model to see whether line profiles consistent with the observations can be produced.

VII. CONCLUSIONS AND SUMMARY

The ultraviolet rocket data presented here indicate that the average density of neutral atomic hydrogen in the direction of γ Cas is $n(\text{H I}) = 0.15 \text{ cm}^{-3}$, while the amount of molecular hydrogen must be less than 2 percent of the atomic density. Weak lines tentatively identified as interstellar C II, N I, and Si II require a velocity distribution where the strengths of the wings are greater than those of the natural damping profile at velocities about $\pm 50 \text{ km sec}^{-1}$ from the line center. Specifically, an exponential profile with a dispersion $\eta = 15 \text{ km sec}^{-1}$ produces good agreement between the ultraviolet line strengths and the expected abundances for δ and π Sco as well as for γ Cas. Furthermore, this velocity distribution could be consistent with both the 21-cm and optical results for the interstellar medium.

Continuous emission by an extensive circumstellar envelope probably explains the weak He I lines and veiled appearance of the visual spectrum of γ Cas. If observations of the Paschen emission show that the envelope is optically thin, then it probably consists of long prominencelike structures or hot clouds which emit a visual continuum. These clumps of matter must be at an electron temperature near 20000° K and must

radiate efficiently at a distance of several stellar radii from the surface. If the envelope is optically thick at all wavelengths, the first step of determining the geometry is more difficult, because a cooler but larger envelope covering a significant fraction of the photosphere could produce the same amount of veiling. The fact that we see broad photospheric lines and a shifted P Cygni C-IV profile provides a rough upper limit of about 50 percent on the area of the photosphere that could be covered by a cool envelope. Also, the inclination of the axis of rotation would be more important, because an optically thick envelope need not radiate isotropically.

I am deeply grateful for the constant encouragement and guidance offered throughout this work by Dr. Donald Morton. Dr. Lyman Spitzer read the manuscript and suggested several improvements. Dr. Edward Jenkins deserves special thanks for his help in the launch preparations and for supplying many computer programs used in the data reduction. Dr. Theodore E. Houck provided ultraviolet spectral scans from the Wisconsin OAO, and Dr. John F. Heard and Mr. Frederick R. Hickok photographed spectra with the David Dunlap telescope.

The rocket payload was fabricated by the Perkin-Elmer Corporation under the direction of Mr. James Plascyk. Mr. William Harter of Princeton and Mr. Timothy Lyons of Perkin-Elmer assisted in preparing the payload for launch. The excellent lithium fluoride overcoatings on the optics were done by Mr. John Osantowski of the Goddard Space Flight Center. The flight of Aerobee 4.268 was sponsored by contract NSR-31-001-901 with the National Aeronautics and Space Administration, and the data reduction on the Princeton computer was partially supported by grant GP-579 from the National Science Foundation.

REFERENCES

- Aller, L. H. 1963, *Astrophysics: The Atmospheres of the Sun and the Stars* (New York: Ronald Press).
 Ambartsumyan, V. A. 1958, *Theoretical Astrophysics* (London: Pergamon Press).
 Baldwin, R. B. 1942, *Sky and Tel.*, 1, No. 9, 5.
 Blaauw, A. 1963, *Basic Astronomical Data*, ed. K. Aa. Strand (Chicago: University of Chicago Press), p. 383.
 Boyarchuk, A. A., and Kopylov, I. M. 1964, *Pub. Crimean Ap. Obs.*, 31, 44.
 Burbidge, E. M., and Burbidge, G. R. 1955, *Ap. J.*, 122, 89.
 Code, A. D., and Bless, R. C. 1970, in *Proc. I.A.U. Symp. No. 36*, ed. L. Houziaux and H. Butler (Dordrecht: D. Reidel Publishing Co.), p. 173.
 Cowley, A. P., and Marlborough, J. M. 1968, *Pub. A.S.P.*, 80, 42.
 Dalgarno, A., and Allison, A. C. 1968, *Ap. J. (Letters)*, 154, L95.
 Deeming, T. J., and Walker, G. A. H. 1967, *Zs. f. Ap.*, 66, 457.
 Edwards, D. L. 1956, *Vistas in Astronomy*, ed. A. Beer (London: Pergamon Press), 2, 1470.
 Gaillard, M., and Hesser, J. E. 1968, *Ap. J.*, 152, 695.
 Goldberg, L., Müller, E. A., and Aller, L. H. 1960, *Ap. J. Suppl.*, 5, 1.
 Gorbatsky, V. G. 1949, *Astr. Zh.*, 26, 307.
 Griem, H. R. 1964, *Plasma Spectroscopy* (New York: McGraw-Hill Book Co.), p. 125.
 Hardorp, J., and Strittmatter, P. A. 1968, *Ap. J.*, 153, 465.
 Henize, K. G., Wray, J. D., and Wackerling, L. R. 1968, *Bull. Astr. Inst. Czechoslovakia*, 19, 279.
 Hofmann, W. 1969, *Zs. f. Naturforschung*, 24, 990.
 Hutchings, J. B. 1970, private communication.
 Iben, I. 1966, *Ap. J.*, 143, 516.
 Jastrow, R. 1965, *Lectures on Space Physics* (lecture notes distributed for the Columbia University Summer Institute in Space Physics).
 Jenkins, E. B. 1970, in *Proc. I.A.U. Symp. No. 36*, ed. L. Houziaux and H. Butler (Dordrecht: D. Reidel Publishing Co.), p. 281.
 Jenkins, E. B., Morton, D. C., and Matilsky, T. A. 1969, *Ap. J.*, 158, 473.
 Kerr, F. J., and Westerhout, G. 1965, *Galactic Structure*, ed. A. Blaauw and M. Schmidt (Chicago: University of Chicago Press), p. 167.
 Lawrence, G. M., and Savage, B. D. 1966, *Phys. Rev.*, 141, 67.
 Lucy, L. B., and Solomon, P. M. 1970, *Ap. J.*, 159, 879.
 Marlborough, J. M. 1969a (informal communication).
 ———. 1969b, *Ap. J.*, 156, 135.
 Merrill, P. W. 1956, *Lines of the Chemical Elements in Astronomical Spectra* (Carnegie Inst. Washington Pub. No. 610).

- Mihalas, D. 1969, *Ap. J. (Letters)*, **156**, L155.
- Moore, C. E. 1945, *A Multiplet Table of Astrophysical Interest* (rev. ed.; Princeton Univ. Obs. Contr. No. 20).
- . 1950, *An Ultraviolet Multiplet Table* (N.B.S. Circ. No. 488, sec. 1).
- . 1965, *N.B.S. National Standard Reference Data Series*, Vol. 3, sec. 1.
- Morton, D. C. 1969a, *Ap. and Space Sci.*, **3**, 117.
- . 1969b, *Ap. J.*, **158**, 629.
- Morton, D. C., Jenkins, E. B., and Bohlin, R. C. 1968, *Ap. J.*, **154**, 661.
- Morton, D. C., Jenkins, E. B., and Brooks, N. H. 1969, *Ap. J.*, **155**, 875.
- Morton, D. C., and Spitzer, L. 1966, *Ap. J.*, **144**, 1.
- Münch, G. 1968, *Nebulae and Interstellar Matter*, ed. B. M. Middlehurst and L. H. Aller (Chicago: University of Chicago Press), p. 365.
- Osterbrock, D. 1957, *Ap. J.*, **125**, 622.
- Savage, B. D., and Lawrence, G. M. 1966, *Ap. J.*, **146**, 940.
- Secchi, A. 1867, *A.N.*, **68**, 63.
- Shelus, P. J. 1967, *Sky and Tel.*, **33**, 220.
- Smith, A. M. 1969, *Ap. J.*, **156**, 93.
- Spitzer, L. 1968, *Diffuse Matter in Space* (New York: Interscience Publishers).
- Spitzer, L., Dressler, K., and Upson, W. L. 1964, *Pub. A.S.P.*, **76**, 387.
- Stone, M. E., and Morton, D. C. 1967, *Ap. J.*, **149**, 29.
- Stothers, R. 1963, *Ap. J.*, **138**, 1074.
- Swings, P., and Struve, O. 1941, *Ap. J.*, **94**, 291.
- Underhill, A. B. 1949, *M.N.R.A.S.*, **109**, 562.
- Van Citters, G. W., and Morton, D. C. 1970, *Ap. J.*, **161**, 695.
- Wentzel, D. 1970, *Ap. J.*, **160**, 373.
- Westerhout, G. 1969, *Maryland-Green Bank Galactic 21-cm Line Survey* (2d ed.; College Park: University of Maryland).
- Wiese, W. L., Smith, M. W., and Glennon, B. M. 1966, *Atomic Transition Probabilities* (Washington: National Bureau of Standards), Vol. 1.
- Wiese, W. L., Smith, M. W., and Miles, B. M. 1969, *Atomic Transition Probabilities* (Washington: National Bureau of Standards), Vol. 2.
- Wilson, R. E. 1953, *General Catalogue of Stellar Radial Velocities* (Carnegie Inst. Washington Pub. No. 601).

